



Available online at www.sciencedirect.com



International Journal of Solids and Structures 43 (2006) 2076–2090

INTERNATIONAL JOURNAL OF
SOLIDS and
STRUCTURES

www.elsevier.com/locate/ijsolstr

Seismic behaviour of industrial masonry chimneys

Francisco J. Pallarés ^{a,*}, Antonio Agüero ^b, Manuel Martín ^a

^a Departamento de Física Aplicada, Universidad Politécnica de Valencia, Camino de Vera, s/n, CP 46022, Valencia, Spain

^b Departamento de Mecánica de los Medios Continuos y Teoría de Estructuras, Universidad Politécnica de Valencia, Camino de Vera, s/n, CP 46022, Valencia, Spain

Received 14 December 2004; received in revised form 4 June 2005

Available online 20 July 2005

Abstract

This paper deals with the seismic behaviour of an unreinforced masonry chimney representative of the large number of chimneys currently in existence in many European areas which were built during the period of the industrial revolution. Maximum seismic intensity value that can be resisted in terms of peak ground acceleration and failure mode are the main goals. A 3D finite element model capable of reproducing cracking and crushing phenomena have been used in a non-linear analysis in order to obtain lateral displacements, crack pattern and failure mode for this type of construction. Earthquakes artificially generated for a low to moderate seismic intensity area from the response spectrum proposed by the codes have been tested on the structure obtaining failure mode, maximum stresses and displacements. Subsequently, the accelerograms generated were scaled until non-failure earthquakes were obtained.

© 2005 Elsevier Ltd. All rights reserved.

Keywords: Masonry; Industrial chimney; Earthquake; Seismic behaviour; Cracking; Crushing; Failure mode; Accelerogram

1. Introduction

The present work focuses on the study of the seismic behaviour of industrial chimneys made of brick-work and mortar which sprung up rapidly throughout many parts of Europe during the period of the industrial revolution (Fig. 1).

These chimneys were built to create the necessary chimney effect and produce the steam boilers combustion of the industries which were flourishing towards the end of the 19th century and the beginning of the 20th century until the 1950s, when electric power substituted this production system.

* Corresponding author. Tel.: +034 96 387 70 07x75236; fax: +034 96 387 71 59.

E-mail address: frapalru@fis.upv.es (F.J. Pallarés).



Fig. 1. Industrial brickwork chimney.

Initially, the chimneys were destined for the textile industry. However, their use was eventually extended to all types of industries such as, for example, those dedicated to the manufacturing of paper.

Despite the number of studies relating to masonry structures in scientific literature is growing, few of them deal with this type of masonry construction. It must be pointed out that the existing literature related to the modelling of this type of structure is rather scarce without any experimental investigation known by the authors. It is therefore appropriate herein to study these constructions since existing knowledge regarding their behaviour is very limited and, in addition, in many places these chimneys are considered the silent witnesses of the past and they are protected by law as cultural heritage.

Some examples of research dealing with this sort of construction can be found in [Riva and Zorgno \(1995\)](#) and [Pistone et al. \(1995\)](#). The first work analyses the typology and structure of industrial chimneys built between 1870 and the first decades of the 20th century in the Italian regions of Piedemont and Veneto. The study also analyses problems associated with their restoration. The second paper studies the behaviour of three significant chimneys in these areas using the finite element method with a linear analysis, taking into account the self-weight of the chimney, wind, temperature differences and earthquakes as acting forces. Moreover, [Pistone et al. \(1996\)](#) deals with restoration problems in masonry chimneys. Recently, two more examples addressing with this type of construction are (a) [Pallarés et al. \(2004\)](#), where different failure criteria are compared to study the failure of a masonry chimney, and (b) [Vermeltfoort \(2004\)](#), in which stability and preservation of these chimneys are treated.

A key feature in the response of these industrial chimneys under the action of different loads, in particular, during earthquake motions, is that they exhibit insufficient tensile strength to perform satisfactorily due to unreinforced masonry was used in the construction. Since many areas located on the Mediterranean coastal area undergo intense, moderate or low seismic activity, this is the basis for the present study, which aims to expand the existing knowledge regarding the seismic behaviour of this kind of masonry structure and to know if measures are needed to protect them in case of earthquake.

An estimation of the strongest earthquake a chimney can withstand, and the behaviour and failure mode of a chimney during a specific seismic action of low or moderate intensity proposed by the European code (Eurocode 8), adapted to the case of the Spanish Mediterranean area (NCSE, 2002), are aspects which will be considered in the present work.

2. Characterization of masonry

As mentioned before, over the last few years, there has been an increasing number of scientific studies aimed at providing a better understanding of the behaviour of masonry since, to date, this ancient material has been considered to be practically unknown due to its constructive variability and the shift in scientific research towards such materials as concrete or steel. Recent examples of masonry studies can be found in: Anthoine (1995), who, using the homogenization theory for periodic materials develops a material model for masonry; Lotfi and Shing (1991) adopt a smeared crack finite element formulation using the J_2 plasticity model for uncracked masonry and non-linear orthotropic constitutive models for cracked masonry; Lourenço et al. (1998) develop a yield criterion with different strengths along each material axis; Ma et al. (2001) using numerical simulations with micromodels and the homogenization technique obtain mechanical characteristics for homogenized masonry.

However, there are few references regarding the study of the dynamic behaviour of masonry: Mendola et al. (1995), analysing the stability condition of masonry walls subjected to seismic transverse forces, reduce this problem to the study of a column undergoing equivalent static horizontal forces; Zughe et al. (1998) carry out a simplified study of the dynamic behaviour of masonry developing a comprehensive analytical model predicting both joint sliding and the cracking and/or crushing failure modes; Lam et al. (2002) using 1-DOF simplified models reproduce the behaviour of masonry walls subject to dynamic actions.

Generally, masonry is a non-homogeneous anisotropic material consisting of units and mortar with an inelastic behaviour. Although there are micromodels which accurately reproduce this complex behaviour of masonry when specific tests are carried out at the laboratory (Lourenço and Rots, 1997), such models based on micromodelization make analysis very complex with a high computational effort, especially for any study of masonry structures discretised by means of a medium-size or large number of finite elements. In order to avoid this difficulty and simplify the problem, since the aim of the work is to investigate the seismic response of a representative unreinforced masonry chimney, a macromodel has been used with a homogeneous material based on an elastic and linear behaviour until cracking or crushing of the material occurs. Following this, a non-linear behaviour is exhibited, and the stiffness matrices are recalculated for the cracked or crushed elements. The type of masonry studied in this paper presents strength properties similar to those found in the material used in the construction of the industrial chimneys of that period, Gouilly (1876).

uniaxial compressive strength: $f_c = 6,376,500 \text{ N/m}^2$

uniaxial tensile strength: $f_t = 196,200 \text{ N/m}^2$

elastic modulus: $E = 5.886 \text{e}9 \text{ N/m}^2$

Poisson coefficient $\nu = 0.2$

density: $\rho = 1600 \text{ kg/m}^3$

These values are important parameters in the resistance to earthquake loads. A low tensile strength has been chosen in order to consider lime mortar used in the first chimneys made in the 19th century and to include chimneys made in cement mortar but with degenerated mechanical properties due to external attacks.

The failure criterion used to separate the linear behaviour from the non-linear behaviour of the material is that proposed by Willam and Warnke (1975) and Pallarés et al. (2004). Thus, when the failure surface is

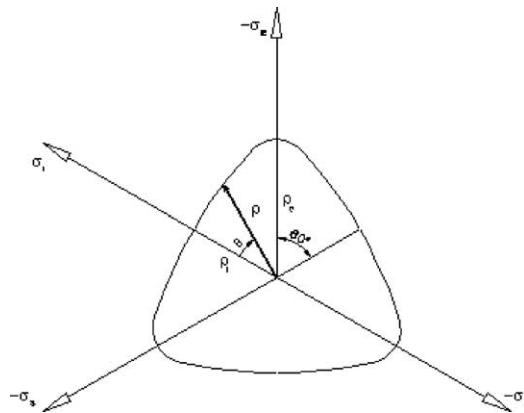


Fig. 2. Deviatoric section of the failure surface.

reached, if one of the principal stresses is a tensile stress, a crack will be developed on the perpendicular plane in the direction marked by this principal tensile stress. However, if all the stresses are compressive stresses, the crushing of the material will follow.

The crushing of the material implies the elimination of the crushed area with regard to the contribution to the stiffness of the element, whereas cracking introduces planes of weakness on the stiffness matrix (depending on the crack, opened or closed, the elastic matrix is adjusted).

The failure surface is (Chen and Saleeb, 1982)

$$f(\sigma_m, \tau_m, \theta) = \sqrt{5} \frac{\tau_m}{\rho(\sigma_m, \theta)} - 1 = 0$$

where

$$\rho(\sigma_m, \theta) = \frac{2\rho_c(\rho_c^2 - \rho_t^2) \cos \theta + \rho_c(2\rho_t - \rho_c) \sqrt{4(\rho_c^2 - \rho_t^2) \cos^2 \theta + 5\rho_t^2 - 4\rho_t \rho_c}}{4(\rho_c^2 - \rho_t^2) \cos^2 \theta + (\rho_c - 2\rho_t)^2}$$

θ is the angle of similarity given by: $\cos \theta = \frac{2\sigma_1 - \sigma_2 - \sigma_3}{2\sqrt{3}\sqrt{J_2}}$; J_2 is the second invariant of stress deviator tensor; $\sigma_1, \sigma_2, \sigma_3$ are the principal stresses; σ_m is the mean normal stress: $\sigma_m = \frac{\sigma_1 + \sigma_2 + \sigma_3}{3}$; ρ_c is the deviatoric length for $\theta = 60^\circ$, and ρ_t is the deviatoric length for $\theta = 0^\circ$; τ_m is the mean shear strength: $\tau_m = \sqrt{\frac{2}{3}J_2}$.

Fig. 2 shows a deviatoric section in principal stresses space.

Although large deflections or large strains are not expected due to structure stiffness and masonry, a non-linear geometric analysis have been performed in order to consider possible $P\text{-}\Delta$ effects.

The structural damping assumed for the masonry structure according to the dynamic calculations carried out is 3% (Paulay and Priestley, 1992).

3. Seismic action

The accelerograms which correspond to the seismic motions considered in the present paper have been artificially generated using the response spectrum proposed in the [Eurocode 8](#) for an area of low-to-moderate seismicity adapted to the Spanish Mediterranean region (Fig. 3) in order to carry out a time-dependent non-linear analysis. However, the methodology used and many of the conclusions drawn can be extended to other seismic zones.

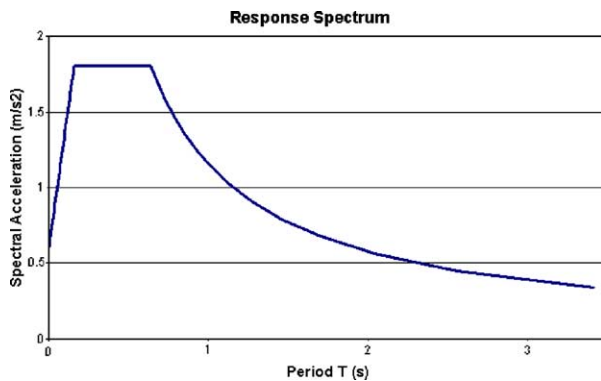


Fig. 3. Response spectrum proposed.

Using the technique proposed by [Gasparini and Vanmarcke \(1976\)](#), five synthetic accelerograms, each compatible with the response spectrum proposed in the mentioned regulations, have been generated and applied to the structure studied in this work. One of these accelerograms, the time integration of which offers the velocities and displacements produced at ground level, is shown in [Figs. 4–6](#).

Since the aim of the paper is the study of the behaviour of the structure and the failure mode in the event of a seismic motion of low to moderate magnitude, the accelerograms, velocities and displacements of the

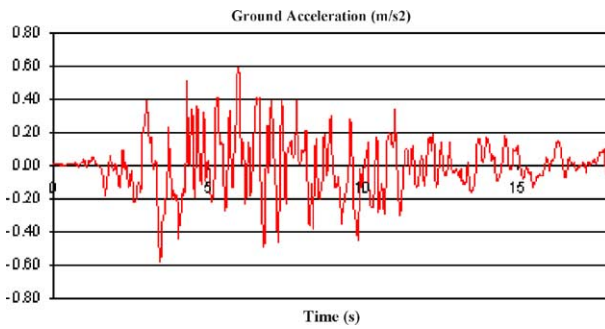


Fig. 4. Accelerogram. Ground acceleration.

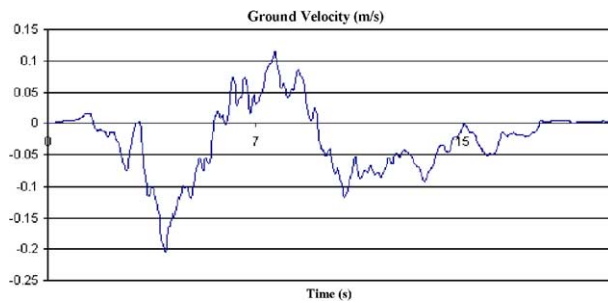


Fig. 5. Ground velocity.

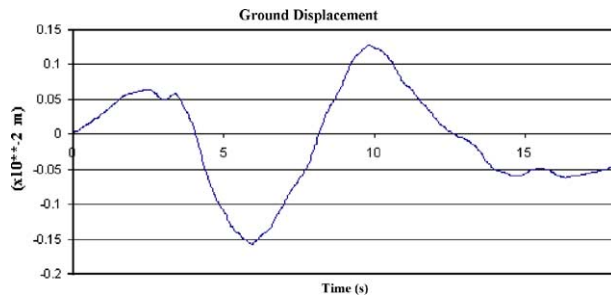


Fig. 6. Ground displacement.

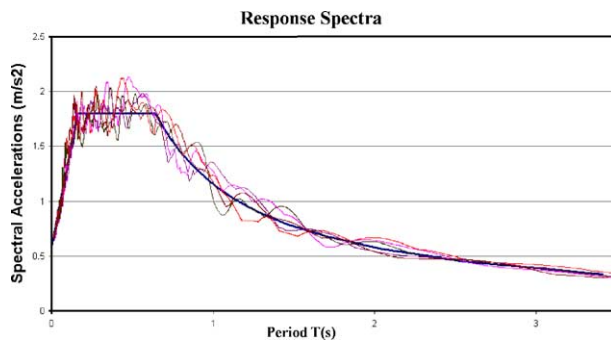


Fig. 7. Accelerations response spectra.

five seismic activities have not been reproduced. However, acceleration response spectra for these five synthetic accelerograms superimposed with the acceleration response spectrum proposed are enclosed in Fig. 7 showing good agreement.

4. Description of the structure

Industrial masonry chimneys dating from the end of the 19th century and the beginning of the 20th century were built to discharge combustion smoke and create the necessary chimney effect (draught) in the industrial procedure. Therefore, they comprised of straight and prismatic forms and their sections generally varied in height.

In the main, they consist of three parts:

- Base: its function is the distribution of the load at the ground level (sometimes nonexistent).
- Shaft: this is the actual chimney.
- Crown: its function is purely ornamental and, as such, is not regarded as a structural element.

The structure studied in the present work is an industrial masonry chimney, the dimensions and circular section of which are representative of the great number of existing chimneys throughout Mediterranean coastal areas and numerous zones within Europe. These dimensions were established by rules dictated by the practice and assembled in different handbooks such as Gouilly (1876) or Esselborn (1928). Although

some variability in the dimensions of different chimneys exists, the ones presented here are considered valid and representative for the purpose of this study, since their variability is not a parameter studied here.

The dimensions of the chimney (in meters) and a cross section at 20 m high are given in Fig. 8. The chimney's internal diameter and wall thickness are assumed to be linearly varying.

Although different models have been developed to represent the seismic behaviour of the chimney (1D, 2D and 3D models), the one most suited to the aim of this study is the 3D model, and therefore, only results for this model will be given.

It will be assumed that the chimney under study does not exhibit structural damage, surface deterioration, cracks or deformations caused by thermal actions.

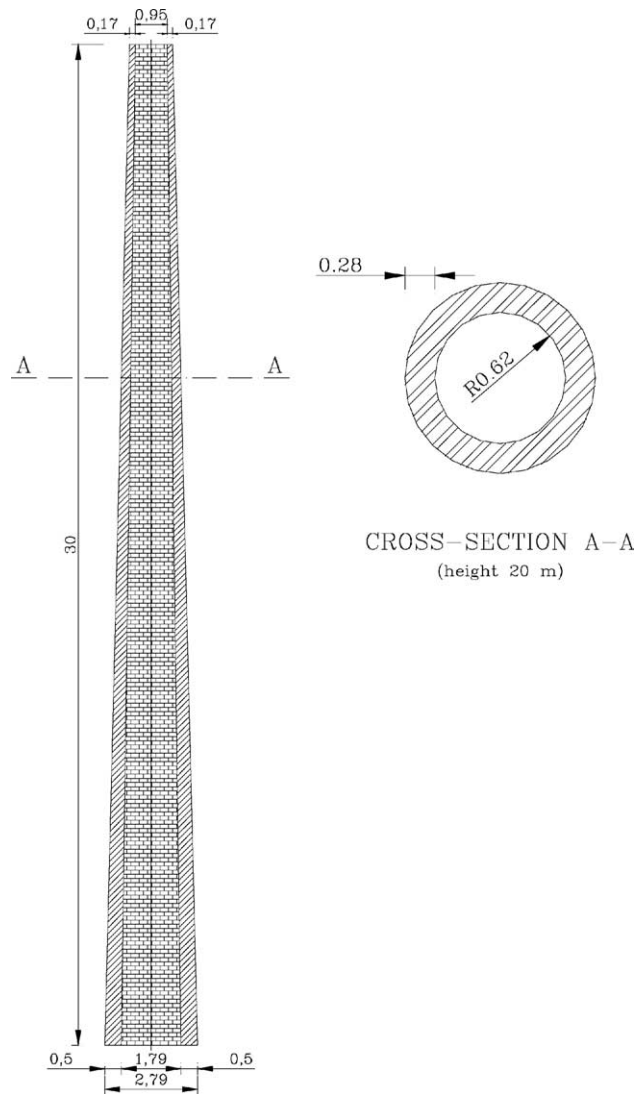


Fig. 8. Longitudinal section and cross-section at 20 m high.

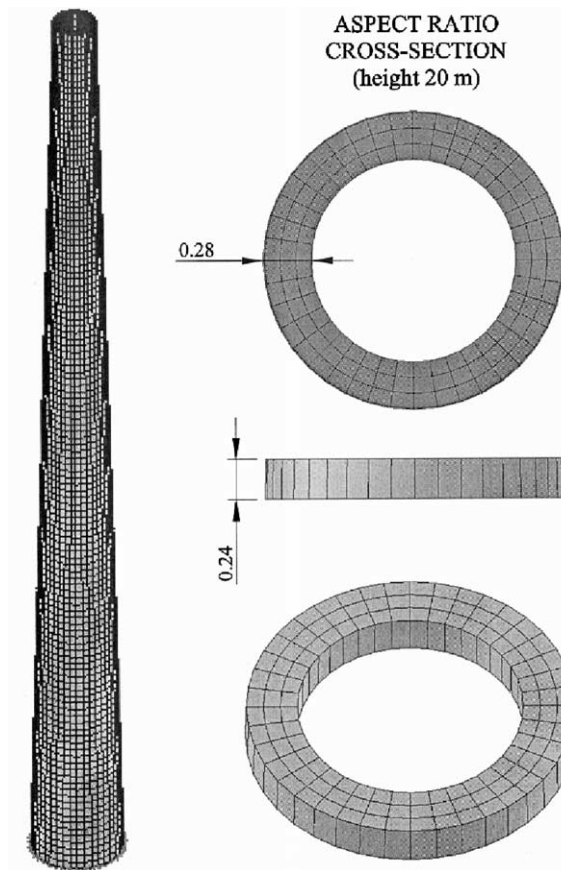


Fig. 9. Finite element model and aspect ratio used in the discretization (cross-section).

The 3D model developed in order to study the seismic behaviour of the chimney is shown in Fig. 9 together with the section at 20 m high to show the aspect ratio used in the model. 3D 8-node hexahedral solid elements with three degrees of freedom per node and eight integration points are displayed. Relating to boundary conditions, displacements at the base of the chimney have been considered fixed in vertical direction. No soil-structure interaction or base rotations have been taken into account.

Thus, using this finite element approach, masonry is modelled as a continuum, and lateral displacements, stresses, crack patterns and failure modes can all be adequately estimated.

5. Results

Using a Pentium IV 2.8 GHz processor with 1 GB RAM, an average of 40 calculation hours were required to achieve the convergence criteria for all the substeps into which the seismic action was divided.

Some results are shown in Fig. 10a and b, in which stresses in masonry for different times during one of the seismic motions can be seen. Usually, the nodes with greater tensile or compressive stresses are located at the base of the chimney. However, there are moments in which a shaft node at a certain height reaches the greatest tensile or compressive stresses.

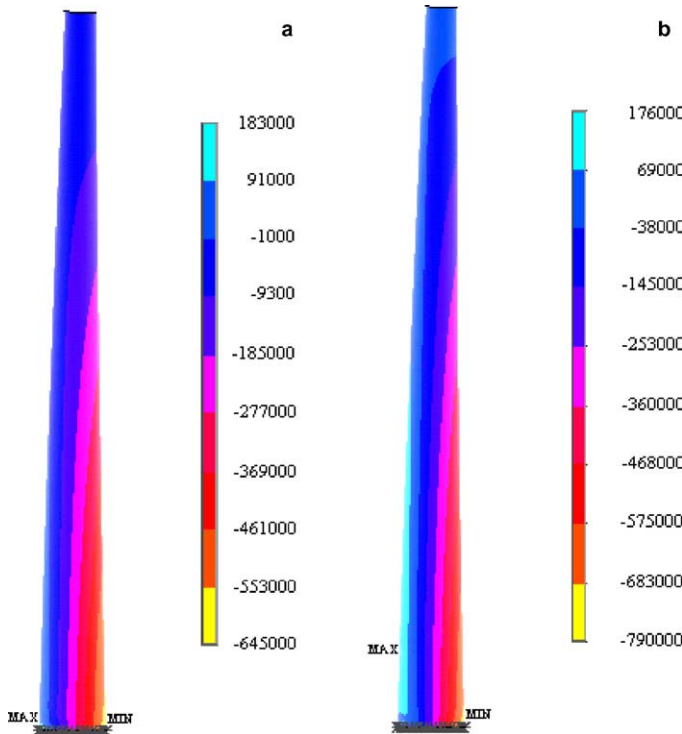


Fig. 10. Longitudinal stress distribution (vertical axis): $t = 3.44$ s (a) and $t = 3.48$ s (b) belonging to one of the seismic actions studied. Frontal view (N/m^2). Maximum tensile stress located at the base of the chimney (a) and at the lower part (b).

For the five accelerograms used, the convergence criteria failed to be reached in a particular time during the seismic motions. This is what in this paper will be referred as “collapse” of the structure, leading to a failure mode of the chimney that cannot resist the seismic action by severe cracking.

Similar results were obtained for the five seismic motions in terms of failure mode. The general crack pattern obtained for these earthquakes before the collapse of the structure is shown in Fig. 11.

The peak ground acceleration which produces this collapse in the chimney is 0.06 g, as can be seen in the response spectrum (Fig. 3).

This peak ground acceleration can be related to earthquake intensity. In spite of the difficulties in correlating this peak ground acceleration to earthquake intensity, some relationships have been reported in Trifunac and Brady (1975) and Murphy and O'Brien (1977). An average relationship of these expressions can be found in Paulay and Priestley (1992):

$$I = (\log_{10} a + 2.4)/0.34$$

where a is the peak ground acceleration in m/s^2 , and I the Modified Mercalli (MM) intensity.

The peak ground acceleration obtained before corresponds to a MM intensity of 6.4 (supposed intensity a continuous scale). Spanish standard correlation produces 6.7.

Regarding seismic magnitude, the relationship is more difficult to formulate. Wang et al. (1979) proposed a table in which an intensity VI–VII corresponds approximately to magnitude 5, and VII–VIII to 6. This value is in accordance with that proposed by Gutenberg and Richter (1942) or Herschberger (1956) obtained with the expressions:

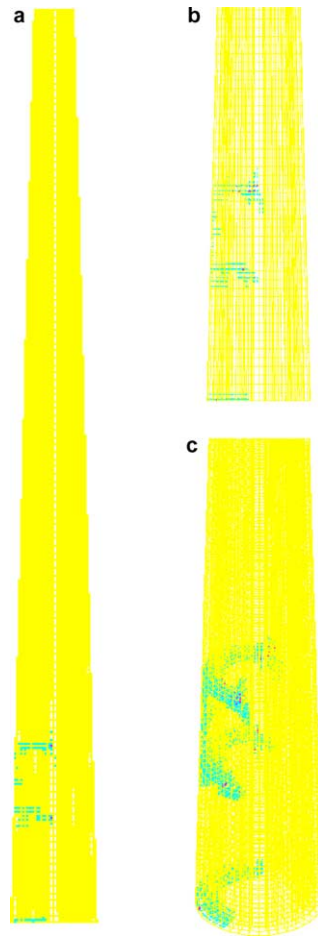


Fig. 11. Crack pattern. Frontal view (a-global, b-base zoom) and oblique view (c-base zoom). Cracks at the base and the lower part of the chimney.

$$I = 1.5 \cdot (M - 1)$$

$$I = 1.67 \cdot M - 2.67 \pm 0.5$$

where M is the magnitude, so the collapse earthquake magnitude would be round 5.3.

6. Non-destructive earthquakes

In the previous figures it has been shown that for all the artificial seismic motions generated to match the intensity proposed by the regulations, cracks have appeared at several points of the chimney since the failure criterion proposed has been reached, leading to the structure collapse in the end. Therefore, in order to know the maximum seismic action that the chimney can withstand without cracking and collapsing, it will be necessary to diminish the intensity of these seismic motions so that new earthquakes, which result in no cracking and collapsing of these industrial chimneys, can be obtained.

By gradually diminishing the seismic intensity for each earthquake until no failure of the chimney is produced, the maximum seismic action in terms of peak ground acceleration that can be resisted is obtained.

Hence, all these new accelerograms are identical in frequency content but they differ in their acceleration values. Although the use of peak ground acceleration to characterize a seismic action gives a poor description of its destructive power, it is normally common used in seismic standards, and in this case, it can be used to compare the initial and the scaled earthquakes.

One of these scaled accelerograms is displayed in Fig. 12 with 0.03 g the peak ground acceleration value:

As previously mentioned, the five earthquakes were scaled and tested until the convergence criteria were fulfilled during the seismic motion. These earthquakes are non-destructive earthquakes, producing no

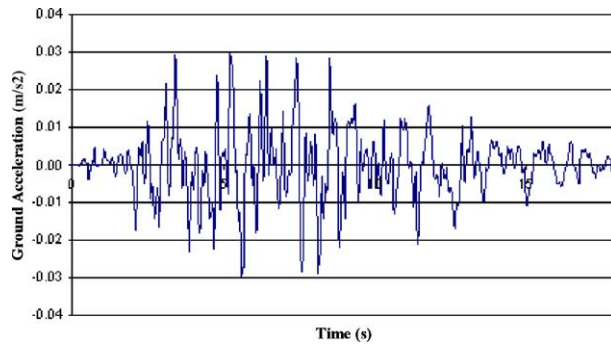


Fig. 12. Scaled accelerogram.

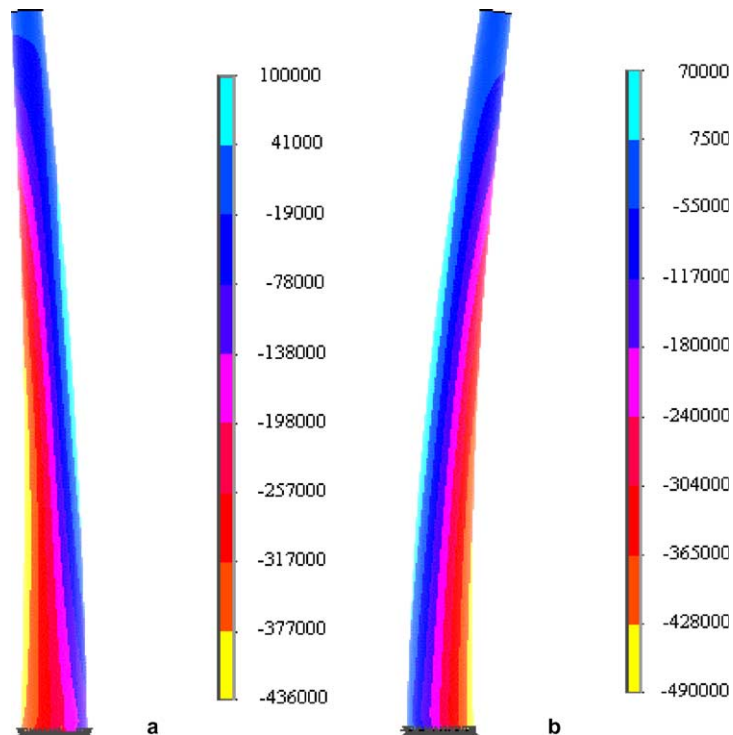


Fig. 13. (a) Longitudinal stress distribution (vertical axis): $t = 5.12$ s. Frontal view (N/m^2). (b) Longitudinal stress distribution (vertical axis): $t = 5.42$ s. Frontal view (N/m^2).

damage with a peak ground acceleration lower than 0.04 g, which corresponds to VI for the intensity value and, approximately, five for the magnitude.

Fig. 13a and b display stress distribution along the chimney belonging to one of the seismic actions studied. The maximum tensile stress is located at the base of the chimney in both cases.

A comparison between stresses for two nodes of the structure which undergo large stresses, one at the base and another at the shaft of the chimney, can be seen in Figs. 14 and 15.

As can be observed from the graphs, while compressive stress reached by the masonry can be withstood without any difficulty, tensile stress is close to the failure criterion. Although the results obtained are for a specific seismic motion, similar graphs can be produced for the rest of the seismic motions studied.

The comparison between the displacements undergone by nodes at the base, which agrees with the imposed seismic motion, and its amplification produced at the crown nodes can be observed in Fig. 16.

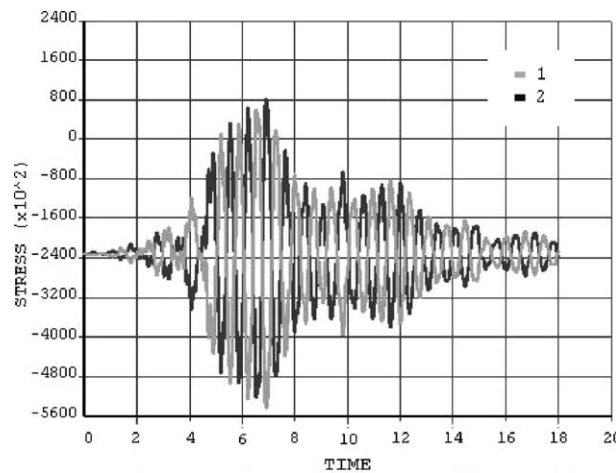


Fig. 14. Longitudinal stresses time-history (vertical axis) for the left and right end nodes of the base section.

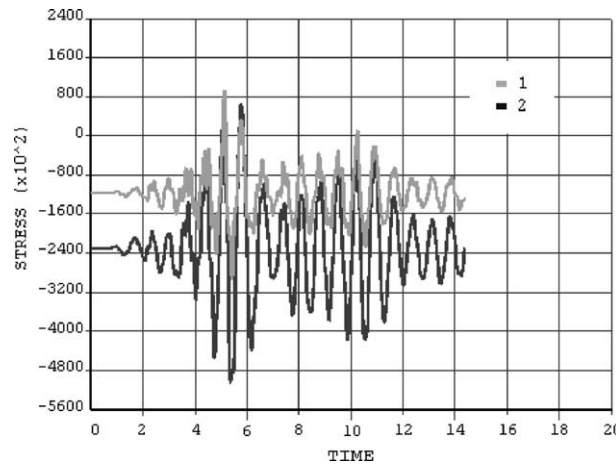


Fig. 15. Longitudinal stresses time-history (vertical axis) for the left end node of the base section (2) and the left end node located at a height of 19.3 m (1).

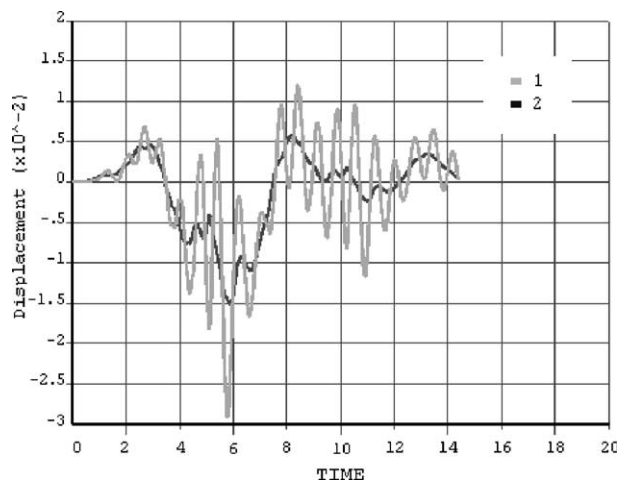


Fig. 16. Horizontal displacements time-history for the bottom right end (base) node (2) and top right end (crown) node (1). The displacement of the base node corresponds to the seismic motion imposed.



Fig. 17. Final state in the chimney for a low intensity earthquake.

The final state of the chimney after the action of a low-intensity seismic motion is shown in Fig. 17. No cracks are developed.

7. Conclusions

This paper presents the failure mode for an unreinforced masonry chimney representative of the large number of chimneys currently in existence in many European areas which were built during the period of the industrial revolution. The model is based on continuum mechanics theory and smeared crack formulation. A failure criterion and a finite element capable of reproducing cracking and crushing phenomena have been used in a non-linear analysis.

The results obtained from the numerical tests presented have shown that the crack pattern under seismic action can be predicted quite accurately with reasonable results, and can be used in the preservation of these chimneys to guarantee their stability in case of an earthquake (peak ground acceleration approx. 0.04 g or greater, seismic intensity approx. VI and magnitude about 5 would start inducing damage in weakened chimneys) by reinforcing those parts which will undergo the greatest damage (located at the base and the lower part of the chimney).

The 3D analysis performed allows to characterize the behaviour of the chimney during a seismic action, including the crack progress over time, the failure mode and the final crack pattern. In addition, the maximum earthquake in terms of peak ground acceleration, MM intensity or magnitude that the chimney can withstand is obtained.

However, this type of modelling is too time consuming. Future investigations using elements or methodologies less time consuming capable of predicting crack pattern and failure modes are required.

In this way, further research is being carried out in order to create response spectra for this type of construction.

References

Anthoine, A., 1995. Derivation of the in-plane elastic characteristics of masonry through homogenization theory. *Int. J. Solids Struct.* 32, 137–163.

Chen, W.F., Saleeb, A.F., 1982. Constitutive equations for engineering materials. *Elasticity and Modeling*, vol. 1. John Wiley & Sons, Inc.

Esselborn, C., 1928. *Tratado General de Construcción. Tomo 1: Construcción de Edificios*. Ediciones G. Gili, S.A.

Eurocode 8. Design provisions for earthquake resistance of structures. Part 1-1: General rules. Seismic actions and general requirements for structures.

Gasparini, D., Vanmarcke, E., 1976. Simulated Earthquake Motions Compatible with Prescribed Response Spectra. Report R76-4 of the Department of Civil Engineering, Massachusetts Institute of Technology, Massachusetts.

Gouilly, A., 1876. *Théorie sur la Stabilité des Hautes Cheminées en Maçonnerie*. J. Dejey & Cia Imprimeurs-editeurs.

Gutenberg, B., Richter, C.F., 1942. Earthquake magnitude, intensity, energy, and acceleration. *Bull. Seismol. Soc. Am.* 32, 163–191.

Herschberger, J., 1956. A comparison of earthquake accelerations with intensity rating. *Bull. Seismol. Soc. Am.* 46, 317–320.

Lam, N.T.K., Griffith, M., Wilson, J., Doherty, K., 2002. Time-history analysis of URM walls in out-of-plane flexure. *Eng. Struct.* 25 (6), 743–754.

Lotfi, H.R., Shing, P.B., 1991. An appraisal of smeared crack models for masonry shear wall analysis. *Comput. Struct.* 41 (3), 413–425.

Lourenço, P.B., Rots, J.G., 1997. Multisurface interface model for analysis of masonry structures. *J. Eng. Mech.* 123 (7), 660–668.

Lourenço, P.B., Rots, J.G., Blaauwendraad, J., 1998. Continuum model for masonry: parameter estimation and validation. *J. Struct. Eng.* 124 (6), 642–652.

Ma, G., Hao, H., Lu, Y., 2001. Homogenization of masonry using numerical simulations. *J. Eng. Mech.* 127 (5), 421–431.

Mendola, L., Papia, M., Zingone, G., 1995. Stability of masonry walls subjected to seismic transverse forces. *J. Struct. Eng.* 121 (11), 1581–1587.

Murphy, J.R., O'Brien, L.J., 1977. The correlation of peak ground acceleration amplitude with seismic intensity and other physical parameters. *Bull. Seismol. Soc. Am.* 67, 877–915.

NCSE, 2002. Norma De Construcción Sismorresistente: Parte General Y Edificación. Ministerio de Fomento (Spanish Standard).

Pallarés, F.J., Agüero, A., Martín, M., Ivorra, S., 2004. Failure mode in a industrial brickwork chimney using different criteria. In: IV International Seminar of Historical on Structural Analysis of Historical Constructions (SAHC'04). A.A. Balkema Publishers.

Paulay, T., Priestley, M.J.N., 1992. Seismic Design of Reinforced Concrete and Masonry Buildings. John Wiley & Sons.

Pistone, G., Riva, G., Zorgno, A.M., 1995. Structural behaviour of ancient chimneys. In: 5th Int. Conf. on Structural Studies, Repairs and Maintenance of Historical Buildings, STREMAH '95. Advances in Architecture Series, vol. 3. Comp. Mech. Publications, Southampton, Boston.

Pistone, G., Riva, G., Zorgno, A.M., 1996. Problems with the restoration of old brickwork chimneys in northern Italy. Proceedings of the 7th International Brick Masonry Conference, vol. 1. University of Notre Dame, South Bend, Indiana, USA.

Riva, G., Zorgno, A.M., 1995. Old brickwork chimneys: structural features and restoration problems. In: 4th Int. Conf. on Structural Studies, Repairs and Maintenance of Historical Buildings, STREMAH '95. Dynamics, Repairs and Restoration, vol. 2. Comp. Mech. Publications, Southampton, Boston.

Trifunac, M.D., Brady, A.G., 1975. On the correlation of seismic intensity with peaks of recorded strong ground motion. Bull. Seismol. Soc. Am. 65, 139–162.

Vermeltoort, A.T., 2004. Preservation and stability of industrial masonry chimneys. In: IV International Seminar of Historical on Structural Analysis of Historical Constructions (SAHC'04). A.A. Balkema Publishers.

Wang, L.R.L., O'Rourke, M.J., Pikul, R.R., 1979. Seismic Vulnerability, Behavior and Design of Underground Piping Systems, Technical Report No. 9, Department of Civil Engineering, Rensselaer Polytechnic Institute, New York.

Willam, K.J., Warnke, E.D., 1975. Constitutive Model for the Triaxial Behavior of Concrete. Proceedings International Association for Bridge and Structural Engineering, vol. 19, ISMES, Bergamo, Italy.

Zughe, Y., Thambiratnam, D., Corderoy, J., 1998. Non-linear dynamic analysis of unreinforced masonry. J. Struct. Eng. 124 (3), 270–277.